

---

# RELIABLE UNCERTAINTY WITH CHEAPER NEURAL NETWORK ENSEMBLES: A CASE STUDY IN INDUSTRIAL PARTS CLASSIFICATION

---

A PREPRINT

 **Arthur Thuy\***  
Ghent University  
CVAMO Core Lab, Flanders Make  
arthur.thuy@ugent.be

 **Dries F. Benoit**  
Ghent University  
CVAMO Core Lab, Flanders Make  
dries.benoit@ugent.be

## ABSTRACT

In operations research (OR), predictive models often encounter out-of-distribution (OOD) scenarios where the data distribution differs from the training data distribution. In recent years, neural networks (NNs) are gaining traction in OR for their exceptional performance in fields such as image classification. However, NNs tend to make confident yet incorrect predictions when confronted with OOD data. Uncertainty estimation offers a solution to overconfident models, communicating when the output should (not) be trusted. Hence, reliable uncertainty quantification in NNs is crucial in the OR domain. Deep ensembles, composed of multiple independent NNs, have emerged as a promising approach, offering not only strong predictive accuracy but also reliable uncertainty estimation. However, their deployment is challenging due to substantial computational demands. Recent fundamental research has proposed more efficient NN ensembles, namely the snapshot, batch, and multi-input multi-output ensemble. This study is the first to provide a comprehensive comparison of a single NN, a deep ensemble, and the three efficient NN ensembles. In addition, we propose a Diversity Quality metric to quantify the ensembles' performance on the in-distribution and OOD sets in one single metric. The OR case study discusses industrial parts classification to identify and manage spare parts, important for timely maintenance of industrial plants. The results highlight the batch ensemble as a cost-effective and competitive alternative to the deep ensemble. It outperforms the deep ensemble in both uncertainty and accuracy while exhibiting a training time speedup of 7x, a test time speedup of 8x, and 9x memory savings.

**Keywords** Neural network ensembles · Computational efficiency · Uncertainty quantification · Out-of-distribution data · Manufacturing

## 1 Introduction

During deployment in operations research (OR), predictive models inevitably encounter scenarios where the data distribution differs from the training data distribution, referred to as out-of-distribution (OOD) data. For instance, in predictive maintenance, unseen operating conditions like higher temperatures or humidity might impact model performance.

In recent years, neural networks (NNs) are rapidly gaining traction in the OR field for their exceptional performance in fields such as image recognition (Madhav et al., 2023; Mena et al., 2023). However, when confronted with OOD data, NNs tend to make confident yet incorrect predictions (Guo et al., 2017). Specifically, an NN classifier may predict an incorrect label despite assigning a high predicted probability to that class. This behavior poses concerns as the model's performance deteriorates over time with more OOD scenarios encountered, without warning the decision maker.

---

\*Corresponding author

Uncertainty estimation provides a solution to overconfident models by capturing the uncertainty in both the data and the model. As such, it communicates when a model’s output should (not) be trusted (Thuy and Benoit, 2023). Therefore, reliable uncertainty quantification is crucial for the safe deployment of NNs in the OR domain.

Deep ensembles, comprising multiple independent NNs, have emerged as a promising approach, offering not only strong predictive accuracy but also reliable uncertainty estimation (Ovadia et al., 2019). Individual members are trained independently on the entire dataset and diversity arises from random weight initializations and sampling mini-batches of data during training. Diversity represents the level of disagreement among ensemble members. In OOD scenarios, deep ensembles raise warnings through increased uncertainty and diversity, facilitating timely human intervention to prevent misclassifications (Thuy and Benoit, 2023).

Despite their strong performance, deploying deep ensembles in practice is challenging due to the significant computational and memory demands. That is, the demands increase linearly with the ensemble size. Computation-wise, each member requires a separate forward pass during training and testing. Memory-wise, each member requires a copy of the NN weights. Allocating such substantial resources causes excessively long runtimes and is hard to justify considering financial constraints and environmental concerns.

Recent fundamental research has proposed more efficient NN ensembles, namely the snapshot ensemble (Huang et al., 2017), batch ensemble (Wen et al., 2020), and multi-input multi-output (MIMO) ensemble (Havasi et al., 2020). This study is the first to provide a comprehensive comparison of a single NN, a deep ensemble, and the three efficient NN ensembles. In addition, we propose a Diversity Quality ( $DQ_1$ ) score to quantify the ensembles’ performance on the in-distribution (ID) and OOD sets in one single metric, as opposed to two separate metrics in current literature. The OR case study discusses industrial parts classification to identify and manage spare parts. This task is crucial for timely maintenance of industrial plants and to avoid downtime. During deployment, classifiers frequently encounter unknown parts not present in the training set, requiring a prompt for human intervention.

Extensive analysis of the case study results illustrates that batch ensemble offers a robust alternative to deep ensemble, delivering superior performance at a fraction of the computational cost. In contrast, snapshot and MIMO ensemble lag behind due to either low predictive performance or poor diversity quality.

The remainder of the paper is organized as follows. Section 2 gives an overview of related work and section 3 presents the efficient ensembling techniques. In Section 4, the case study in industrial parts classification is presented. Section 5 gives the results and discussion and presents the Diversity Quality score. Finally, section 6 provides a conclusion.

## 2 Related Work

Related work in OR uses NN ensembles to either improve the predictive performance or to quantify uncertainty. This section describes the literature in both streams.

### 2.1 Ensembles for improved predictive performance

Ensembles have been primarily used to improve the predictive performance of a machine learning system. The individual ensemble members are combined by averaging or majority voting the predictions of all members. Averaging over  $M$  members goes as follows:

$$p(\mathbf{y}^* | \mathbf{x}^*) \approx \frac{1}{M} \sum_{m=1}^M p(\mathbf{y}^* | \mathbf{x}^*, \boldsymbol{\theta}_m). \quad (1)$$

NNs have been widely used as an ensemble member in heterogeneous ensembles, together with other machine learning models such as Lasso regression, XGBoost, and Support Vector Machines. Literature ranges over multiple fields, from finance (Du Jardin, 2021; Cui et al., 2022; Zhang et al., 2023; Jiang et al., 2022; Zhang et al., 2022; Li and Chen, 2021; Krauss et al., 2017) over healthcare (Abedin et al., 2021; Baradaran Rezaei et al., 2023) and manufacturing (Yang et al., 2021; Wu et al., 2022), to politics (Easaw et al., 2023).

Homogeneous ensembles of NNs have also been applied in OR. Relevant literature is in customer service (Zicari et al., 2022), healthcare (Poloni et al., 2022), project tendering (Bilal and Oyedele, 2020), manufacturing (Gupta et al., 2023), and tourism (Pitakaso et al., 2023). The studies find that by combining the outputs of several NNs, an ensemble can outperform any of its members. However, this body of literature is smaller than heterogeneous ensembles, possibly due to the high computational overhead of training multiple NNs.

## 2.2 Ensembles for improved uncertainty quantification

In addition to having strong predictive performance, deep Ensembles have also been shown to exhibit reliable uncertainty estimates (Lakshminarayanan et al., 2017). Uncertainty arises from two sources: data and model uncertainty (Der Kiureghian and Ditlevsen, 2009). Data uncertainty refers to the notion of randomness and is related to the data-measurement process. This uncertainty is irreducible even if more data is collected. Model uncertainty accounts for uncertainty in the model parameters, i.e., uncertainty about which model generated the collected data. In contrast to data uncertainty, collecting more data can reduce model uncertainty. Both types of uncertainty can then be summed to compute the total uncertainty in a prediction.

First, total uncertainty and data uncertainty are approximated using classical information-theoretic measures; then model uncertainty is obtained as the difference (Depeweg et al., 2018):

$$u_{total}(\mathbf{x}^*) \approx H \left[ \frac{1}{M} \sum_{m=1}^M p(\mathbf{y}^* | \mathbf{x}^*, \boldsymbol{\theta}_m) \right] \quad (2)$$

$$u_{data}(\mathbf{x}^*) \approx \frac{1}{M} \sum_{m=1}^M H [p(\mathbf{y}^* | \mathbf{x}^*, \boldsymbol{\theta}_m)] \quad (3)$$

$$u_{model}(\mathbf{x}^*) = u_{total}(\mathbf{x}^*) - u_{data}(\mathbf{x}^*). \quad (4)$$

Total uncertainty is computed by averaging the predictive distributions over the different members and calculating the entropy  $H$ . Data uncertainty is computed by calculating the entropy in each member and averaging the entropies. Intuitively, data uncertainty measures uncertainty in the softmax classification on individual members; model uncertainty measures how much the members deviate. Naturally, the single NN has zero model uncertainty by definition because it only consists of one member. For a classification problem with  $K$  classes, the maximum uncertainty in a prediction is  $\log(K)$ .

Uncertainty quantification is underinvestigated in OR with a limited body of literature. Deep ensembles have been used by Thuy and Benoit (2023); Han and Li (2022); Kim et al. (2023); Prasad et al. (2024); Wen et al. (2022) in the context of OOD detection. Predictions with high uncertainty indicate that the observations lie outside the training data distribution. As such, these predictions are discarded and the observations are passed on to a human expert for a label. Note that Wen et al. (2022) use a snapshot ensemble, although its performance is not compared to other ensemble techniques or a single NN. Furthermore, Zou and Chen (2021) use deep ensembles in active learning. Observations in the unlabeled set causing high model uncertainty are interesting to label. That is, these observations lie outside the current training data distribution and can reduce the model uncertainty once added to the labeled training set.

Kraus et al. (2020) report that the lack of uncertainty quantification in single NNs is a key limiting factor for adoption in the field of OR. The reliable uncertainty estimates from deep ensembles could increase the relevance of NNs, highlighting the need for more efficient NN ensembles.

## 3 Efficient Ensembling Techniques

This section describes the three efficient ensemble techniques that address the computational burden of deep ensembles. Table 1 gives an overview of their improvements over deep ensembles.

Table 1: Overview of efficient NN ensembles, relative to deep ensemble

Ensemble type	Faster training	Faster evaluation	Less memory
Deep ensemble			
Snapshot ensemble	✓		
Batch ensemble	✓	✓	✓
MIMO ensemble	✓	✓	✓

### 3.1 Snapshot ensemble

Snapshot ensemble (Huang et al., 2017) trains a single NN and saves the model parameters at different points in time during training. A cyclic learning rate schedule is used to alternate between converging to local minima and jumping to other modes in the loss landscape (Figure 1). At each local minimum, the weights are saved and a new ensemble

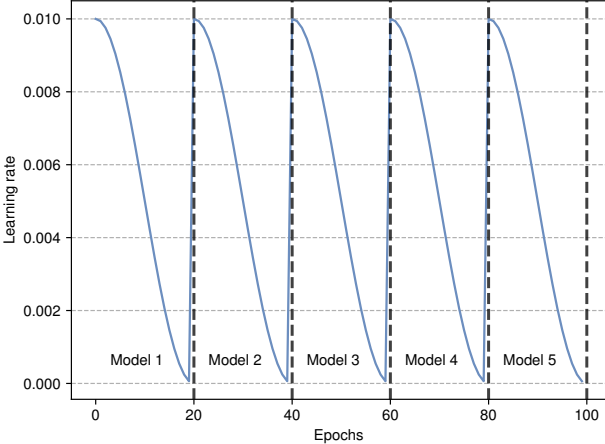


Figure 1: Snapshot ensemble

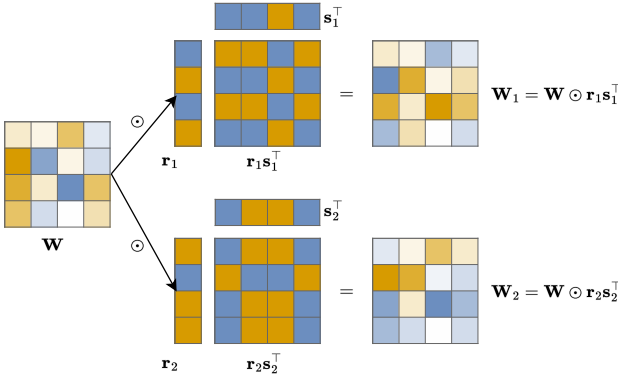


Figure 2: Batch ensemble (adapted from Wen et al. (2020))

member is acquired. Model states taken early in the training process have high diversity but poor accuracy, while model states taken later in the training process tend to have high accuracy but are more correlated. The idea is that the combination of those multiple optima will produce better results than the final model.

The maximum learning rate controls how far the optimizer jumps to another mode after a restart. Note that the learning rate schedule is determined by the procedure and cannot be combined with another custom learning rate schedule. The selected number of ensemble members directly affects the training time of each member; too many members damages their individual accuracy while too few members negatively affects the uncertainty estimates.

The snapshot ensemble has the same training time than a single NN. However, similar to deep ensembles, the memory cost and the computational cost at test time increase linearly with the amount of ensemble members.

### 3.2 Batch ensemble

Instead of storing a separate weight matrix for each ensemble member, batch ensemble (Wen et al., 2020) decomposes the weight matrices into element-wise products of a shared weight matrix and a rank-1 matrix for each ensemble member (Figure 2). Let  $\mathbf{W} \in \mathbb{R}^{m \times n}$  denote the weights in a NN layer with input dimension  $m$  and output dimension  $n$ . The ensemble size is  $M$  and each ensemble member has weight matrix  $\mathbf{W}_i$ . Each member owns trainable vectors  $\mathbf{r}_i$  and  $\mathbf{s}_i$  which have the same dimension as input  $m$  and output  $n$ , respectively. Batch ensemble generates the ensemble weights  $\mathbf{W}_i$  as follows:

$$\mathbf{W}_i = \mathbf{W} \odot \mathbf{F}_i, \text{ where } \mathbf{F}_i = \mathbf{r}_i \mathbf{s}_i^T, \tag{5}$$

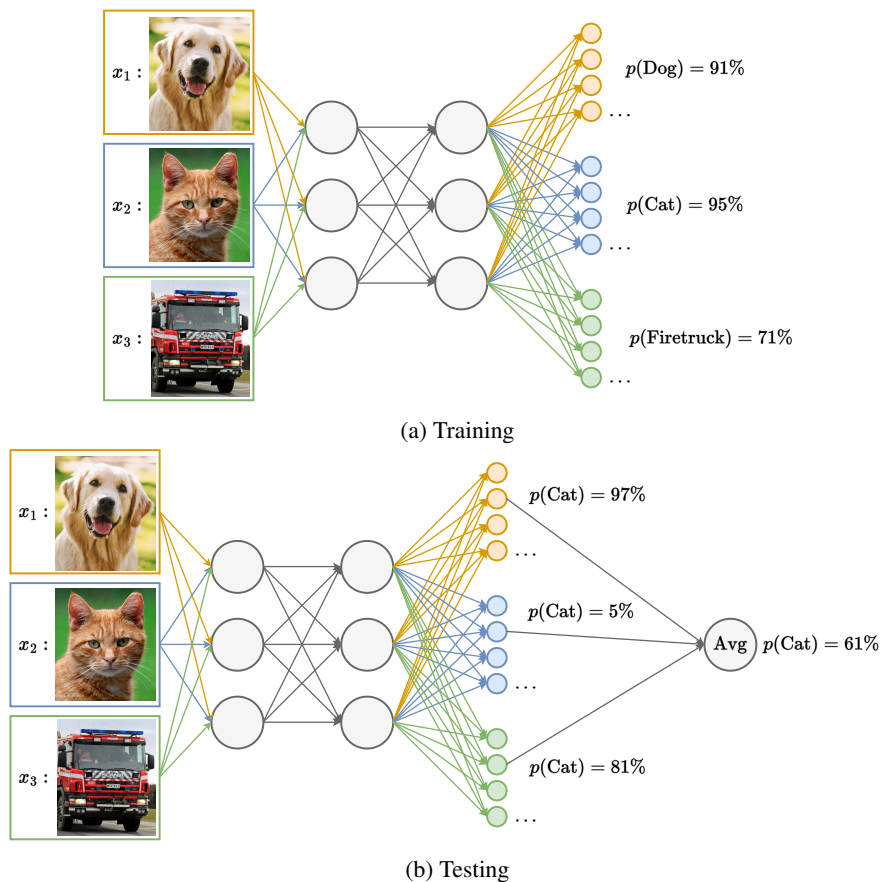


Figure 3: MIMO ensemble at train and test time (adapted from Havasi et al. (2020))

where  $\odot$  denotes an element-wise multiplication.  $\mathbf{W}$  is referred to as the *slow* or *shared* weight because it is shared among all ensemble members, and  $\mathbf{F}_i$  are the *fast* weights. During training and testing, the mini-batch is repeated  $M$  times which enables all ensemble members to compute the output of the same input data points in one single forward pass.

The fast weights can be initialized with either a random signed vector or a random Gaussian vector. Wen et al. (2020) note that the random signed vector often results in higher diversity among the members. In theory, more ensemble members give better results but a higher computational cost; in this sense it is similar to deep ensemble.

Compared to a single NN, the element-wise product during training and testing is the only additional computation that batch ensemble requires, which is cheap compared to a matrix multiplication. With respect to memory, the vectors  $\{\mathbf{r}_1, \dots, \mathbf{r}_m\}$  and  $\{\mathbf{s}_1, \dots, \mathbf{s}_m\}$  are required, which again is cheap compared to full weight matrices.

### 3.3 Multi-Input multi-Output (MIMO) ensemble

MIMO ensemble (Havasi et al., 2020) builds on the idea of sparsity, as it has been shown that 70–80% of the NN connections can be pruned without affecting predictive performance (Zhu and Gupta, 2017). As such, the MIMO ensemble concurrently trains multiple independent subnetworks within one network, without explicit separation.

The MIMO configuration with  $M$  members requires two changes to the NN architecture (Figure 3). First, the input layer is replaced, taking  $M$  datapoints instead of a single datapoint. Second, the output layer is replaced, consisting of  $M$  classification heads based on the last hidden layer instead of a single head. During training, the  $M$  inputs are sampled independently from the training set and each of the  $M$  heads are trained to predict its matching input. At test time, the same input is repeated  $M$  times, causing the heads to make  $M$  independent predictions on the same input, effectively forming an ensemble.

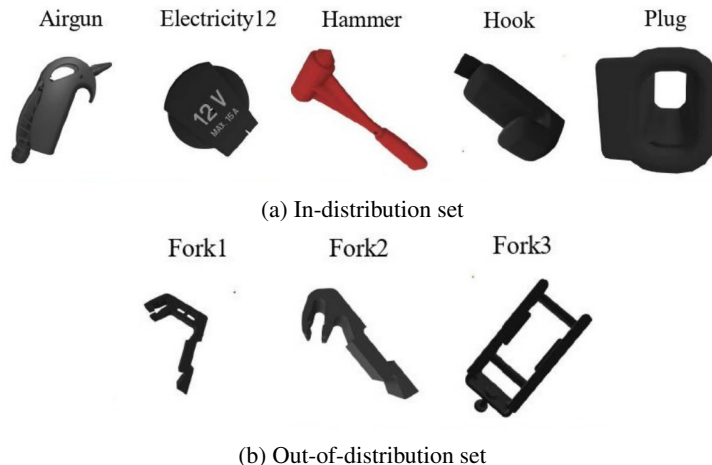


Figure 4: Example observations for the SIP-17 dataset

The number of ensemble members directly affects the number of relationships that need to be learned, which determines the capacity of the subnetworks. Too many members might make the NN capacity prohibitively small with poor accuracy as a result; too few members will cause poor diversity. Havasi et al. (2020) report that 3–4 ensemble members is typically optimal. Additionally, the independence between inputs can be relaxed so that subnetworks can share features. Relaxing independence might particularly benefit networks with limited excess capacity. Increasing the input repetition probability improves the predictive performance but negatively impacts the diversity.

The memory and computation cost of the MIMO ensemble is marginally higher than a single NN due to the larger input and output layer. As such, training, evaluation, and memory costs are slightly higher.

## 4 Case Study: Industrial Parts Classification

### 4.1 Problem setting

Industrial parts classification is crucial for inventory control of spare parts and for maintaining the smooth operation of industrial plants. Spare parts, essential for timely maintenance of industrial plants, constitute a significant portion of inventory stocks (Hu et al., 2017). According to Hu et al. (2015), operational and maintenance support expenses often represent over 60% of the total costs in industrial settings, with spare parts alone accounting for 25–30%. In large enterprises, the inventory can reach tens of thousands of items (Ernst and Cohen, 1990), making it impractical for human operators to manually identify each part and its appropriate inventory strategy. Industrial parts classification offers a solution by enabling the identification and management of spare parts efficiently.

During deployment, a parts classifier is likely to encounter unknown parts not present in the training data. This might occur, for instance, if new parts are introduced after the classifier’s training phase or if it encounters parts handled by departments not included in the initial training data. It is imperative that the classifier can identify these novel situations and signal a warning, prompting human intervention, rather than making incorrect predictions with high confidence.

We apply the efficient ensembling techniques to a dataset for industrial parts classification, investigating their predictive performance and uncertainty estimates, along with their computational expense. Furthermore, we compare the results to those obtained from a single NN and a deep ensemble. The models are trained and subsequently evaluated on (i) an ID test set comprising the same objects and (ii) an OOD set containing entirely different objects.

### 4.2 Data

We use the Synthetic Industrial Parts (SIP-17) dataset (Zhu et al., 2023, cases 1 and 2), a dataset containing images of various industrial parts. The ID set consists of five industrial parts labeled “Airgun,” “Electricity12,” “Hammer,” “Hook,” and “Plug,” while the OOD set consists of three industrial parts labeled “Fork1,” “Fork2,” and “Fork3” (Figure 4).

The ID set is split in a training (70%), validation (15%), and test set (15%). The OOD set is entirely used as test set (i.e., 100%). The dataset is normalized to the [0,1] range, resized to  $32 \times 32$  pixels, and converted to grayscale. During training, data augmentation is applied with random horizontal and vertical flips.

### 4.3 Models

Throughout the experiments, the base model is a LeNet-5 with 80,865 parameters in the standard configuration. All models except the snapshot ensemble are trained using the Adam optimizer with an initial learning rate of 0.001; the snapshot ensemble uses the custom cyclic learning rate schedule with a maximum learning rate of 0.001. The single model, deep ensemble, and snapshot ensemble are trained for 200 epochs. Following Nado et al. (2021), the batch ensemble and MIMO ensemble are trained for 25% longer (i.e., 250 epochs) because they take longer to converge. All models are trained with a batch size of 512. The batch ensemble uses random signed vectors for the fast weights. The MIMO ensemble uses an input repetition probability of 0.8. The deep, snapshot, and batch ensemble have 10 ensemble members. In contrast, the MIMO ensemble only has 4 members as the capacity of the individual members is otherwise too limited. For completeness, Appendix A compares results between MIMO ensembles comprising 4 and 10 members, while Appendix B shows results when all ensembles consist of 4 members.

The models are implemented in TensorFlow using the Uncertainty Baselines repository (Nado et al., 2021) and are trained on an NVIDIA RTX A5000 card. The results are averaged over 5 independent runs with random seeds for a total runtime of 8 hours.

### 4.4 Evaluation metric: Diversity Quality

To gain a deeper understanding of the ensembling techniques, we assess the diversity among ensemble members. The diversity metric measures the fraction of test data points on which predictions of ensemble members disagree (Fort et al., 2019). This metric is 0 when two members make identical predictions and 1 when predictions differ on every example in the test set. As the base model for diversity computation, we average the output distributions over the members and determine the resulting predicted label. The diversity score is related to the model uncertainty in section 5.2 and allows to assign a score to each member.

We propose a novel Diversity Quality ( $DQ_1$ ) score to represent the diversity on both the ID and OOD set in one single metric, made available in the Python package `reject` (Thuy and Benoit, 2024). The ID diversity (IDD) should be as close as possible to 0.0 and the OOD diversity (OODD) as close as possible to 1.0. The  $DQ_1$ -score is the harmonic mean of  $(1 - \text{IDD})$  and OODD, displayed in Equation 6. The harmonic mean assigns equal weights to both IDD and OODD and is most appropriate to handle ratios (Agrawal et al., 2010). It has a minimum value of 0.0 and a maximum value of 1.0. The new evaluation score has the advantage of being close to 0.0 when either the IDD or OODD is poor, while at the same time, the score is close to 1.0 only when both the IDD and OODD are strong.

$$DQ_1 = 2 \cdot \frac{(1 - \text{IDD}) \cdot \text{OODD}}{(1 - \text{IDD}) + \text{OODD}} \quad (6)$$

Being a harmonic mean, it is similar in construction to the  $F_1$ -score between precision and recall often used in machine learning literature (Sokolova and Lapalme, 2009). The  $DQ_1$ -score can also be generalized to a  $DQ_\beta$ -score, valuing one of ID diversity or OOD diversity more than the other. With  $\beta$  a positive real factor, OODD is considered  $\beta$  times as important as IDD:

$$DQ_\beta = (1 + \beta^2) \cdot \frac{(1 - \text{IDD}) \cdot \text{OODD}}{\beta^2 \cdot (1 - \text{IDD}) + \text{OODD}} \quad (7)$$

For  $\beta = 1$ , Equation 7 evaluates to Equation 6. For example, for  $\beta = 2$ , OODD is twice as important as IDD; for  $\beta = 0.5$ , IDD is twice as important as OODD.

## 5 Results and Discussion

### 5.1 In-distribution performance

We evaluate the classification accuracy and the negative log-likelihood (NLL) for the ID predictions. The NLL is commonly used to measure the quality of the model’s uncertainty (Ovadia et al., 2019); lower scores are better. For ensembles, predictions are averaged over the members before metrics are calculated. We expect the ensemble methods to perform better than the single NN. Table 2 shows the results.

In terms of accuracy, the deep ensemble demonstrates a significant performance advantage over the single model. Among the efficient ensembles, the snapshot ensemble falls short, exhibiting substantially poorer performance compared to the single model. Conversely, the batch ensemble displays robust performance and even surpasses the deep ensemble. The MIMO ensemble achieves a slightly lower accuracy than the single model. Similar conclusions hold for the NLL

Table 2: Performance on the ID set

Model	Accuracy (%) $\uparrow$	NLL $\downarrow$
Single	96.61 $\pm$ 0.18	0.1121 $\pm$ 0.0039
Deep E ( $M = 10$ )	98.12 $\pm$ 0.13	0.0695 $\pm$ 0.0024
Snapshot E ( $M = 10$ )	94.69 $\pm$ 0.47	0.1774 $\pm$ 0.0096
Batch E ( $M = 10$ )	98.79 $\pm$ 0.11	0.0499 $\pm$ 0.0029
MIMO E ( $M = 4$ )	95.96 $\pm$ 0.44	0.1168 $\pm$ 0.0092

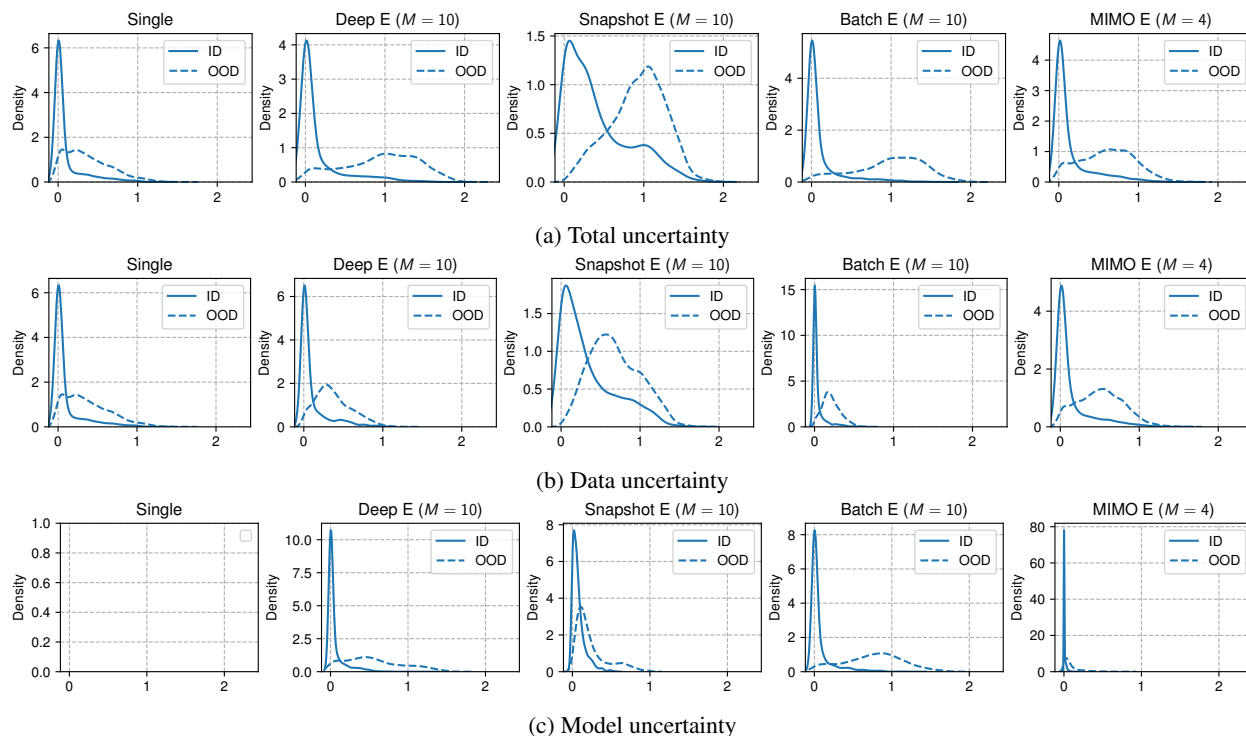


Figure 5: Densities for the data, model, and total uncertainty on the ID and OOD set

metric, where once again, the batch ensemble outperforms the deep ensemble. A lower NLL score indicates a closer alignment of predicted probabilities with the true labels. Overall, the batch ensemble presents highly promising results on the ID set, surpassing the benchmark set by the deep ensemble. Subsequent sections will delve into the OOD behavior of the models.

## 5.2 Uncertainty density

Figure 5 illustrates the density of total, data, and model uncertainty. The results are obtained by evaluating the models on the ID and OOD set, and calculating the uncertainty in each prediction. Note that total uncertainty is the sum of data and model uncertainty and has a maximum value of  $\log_2(5) = 2.32$ . We do not use the NLL here because this requires ground truth labels unavailable for the OOD set. On the ID data, we would like to see low total uncertainty. Conversely, on OOD data, we expect the models to exhibit higher model uncertainty and thus total uncertainty, reflecting an awareness that they know what they do not know. In a highly idealized scenario, the mode of the total uncertainty lies around zero for the ID set and approaches the maximum value of 2.32 for the OOD set.

The single model displays low uncertainty on the ID set but only slightly higher uncertainty on the OOD set. Notably, this uncertainty stems solely from data uncertainty with a mode around 0.2, as the single model lacks the ability to capture model uncertainty. In contrast, the deep ensemble aligns with expectations, demonstrating low uncertainty on the ID set and substantial model uncertainty on the OOD set, resulting in higher total uncertainty with a mode around value 1.0.

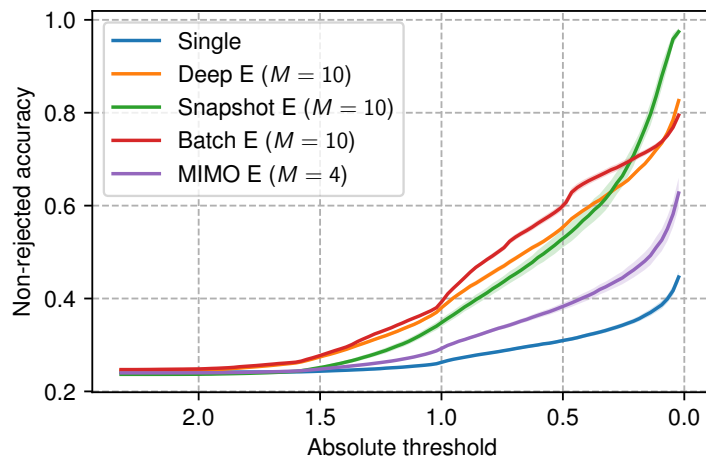


Figure 6: Non-rejected accuracy

Among the efficient ensembles, we observe significant variations in uncertainty behavior. The snapshot ensemble exhibits surprisingly high total uncertainty on the ID set, resulting from high data uncertainty which is undesirable. Furthermore, it has higher total uncertainty on the OOD set with a mode around 1.0 but this primarily stems from data uncertainty, not model uncertainty. The batch ensemble performs well, mirroring the behavior of the deep ensemble with low uncertainty on the ID set and increased model uncertainty on the OOD set with a mode around 1.2. Lastly, the MIMO ensemble indicates low uncertainty on the ID set but falls short on the OOD set. Here, the OOD set induces higher data uncertainty while model uncertainty only experiences a slight increase. Consequently, the total uncertainty on the OOD set has a mode around value 0.75, which is limited compared to other ensemble techniques.

Overall, the batch ensemble once again stands out as the most promising, exhibiting similar uncertainty behavior to the Deep ensemble. Conversely, the snapshot and MIMO ensemble do not show substantially increased model uncertainty on the OOD set.

### 5.3 Classification with rejection

In practical scenarios, it is crucial for a model to avoid overly confident yet incorrect predictions. One method to address this involves passing predictions with high uncertainty to human experts for labeling, known as classification with rejection (Barandas et al., 2022). To assess the ensembles’ uncertainty estimates, accuracy is computed only for observations with a total uncertainty value below a user-defined threshold, referred to as non-rejected accuracy (NRA).

We evaluate the models on the combination of the ID and OOD test sets. A model proficient in identifying OOD data exhibits an NRA curve closer to the top-left corner. Essentially, as the NRA curve rises earlier, the model demonstrates higher uncertainty on observations that in fact prove to be OOD data. Consequently, it prioritizes rejecting OOD observations, then misclassified ID observations, and finally correctly classified ID observations at lower uncertainty levels. Figure 6 displays the NRA for all models based on their total uncertainty.

The single model exhibits the weakest performance, characterized by a slow increase in NRA, reaching only 40% at low uncertainty thresholds. This finding aligns with the low uncertainty observed on the OOD set in Figure 5. In contrast, the deep ensemble demonstrates significantly better performance, showing a much earlier and sharper increase in NRA, reaching 80% at low uncertainty thresholds.

The snapshot ensemble slightly underperforms the deep ensemble until a threshold of 0.25; it is only for smaller uncertainty thresholds that snapshot ensemble has a rapid improvement in NRA. The batch ensemble demonstrates strong performance, outperforming the deep ensemble across the entire range of thresholds. Conversely, the MIMO ensemble disappoints with a slowly increasing NRA, placing it between the single model and deep ensemble.

In summary, the single model produces confident incorrect predictions, as indicated by the low NRA curve. The deep ensemble is substantially better at identifying and rejecting OOD observations, demonstrated by its early and steep increase in NRA. Both the snapshot and batch ensemble perform well and match or even improve on the deep ensemble. Unfortunately, the MIMO ensemble falls short of achieving equally strong NRA values.

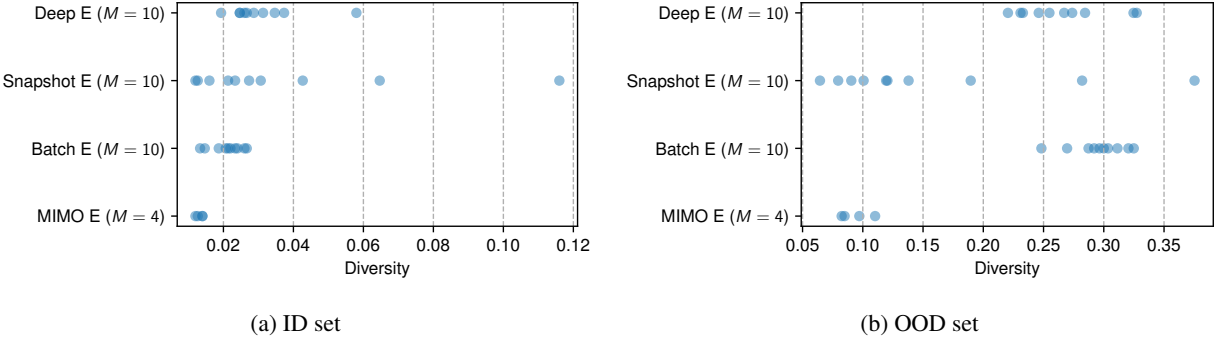


Figure 7: Diversity on the ID and OOD set. Each point represents the diversity of a trained model against the model averaged over all members

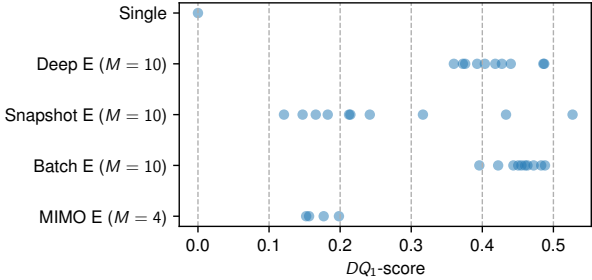


Figure 8:  $DQ_1$ -scores. Each point represents the  $DQ_1$ -score of an ensemble member

### 5.4 Diversity analysis

Figure 7 displays a scatterplot of diversity scores on the ID and OOD test set, where each point represents an ensemble member. Recall that we want low diversity on the ID set and high diversity on the OOD set.

On the ID set (Figure 7a), the MIMO ensemble performs best and has the lowest diversity, followed by the batch ensemble. Both the snapshot and deep ensembles demonstrate slightly higher diversity scores. Notably, the snapshot ensemble displays a skewed diversity distribution, with several members exhibiting significantly higher diversity than the majority. This behavior stems from the initial snapshots being highly diverse, gradually converging as training progresses.

Moving to the OOD set (Figure 7b), the diversity scores are indeed orders of magnitude higher. Here, the MIMO ensemble still has the lowest diversity, which is undesirable as the diversity should be as high as possible on the OOD set. The batch ensemble has the highest diversity and performs strongest, closely followed by the deep ensemble. Again, the snapshot ensemble has generally low diversity, with early snapshots being very diverse.

Examining the ID and OOD scenarios independently poses difficulties in obtaining a comprehensive view of diversity performance. The proposed metric, Diversity Quality ( $DQ_1$ ), addresses this issue and enables a clear assessment of diversity performance across various ensembles.

Figure 8 shows the  $DQ_1$ -scores for each ensemble and its members. The batch ensemble stands out with the highest  $DQ_1$ -scores, attributed to its relatively low IDD and high OODD. The deep ensemble follows closely behind with marginally lower scores than the batch ensemble because of slightly higher IDD and lower OODD. Furthermore, the snapshot ensemble again exhibits a skewed distribution of scores due to its unique training dynamics. The MIMO ensemble ranks lowest in  $DQ_1$ -scores because of its undesirable low OODD, although it has advantageous low IDD. This lack of diversity is reflected in its overall poor  $DQ_1$ -scores. Note that the single NN has a minimum score of zero because it only has one member, thereby lacking diversity altogether. Overall, the  $DQ_1$ -scores comprehensively evaluate the ensembles’ diversity performance.

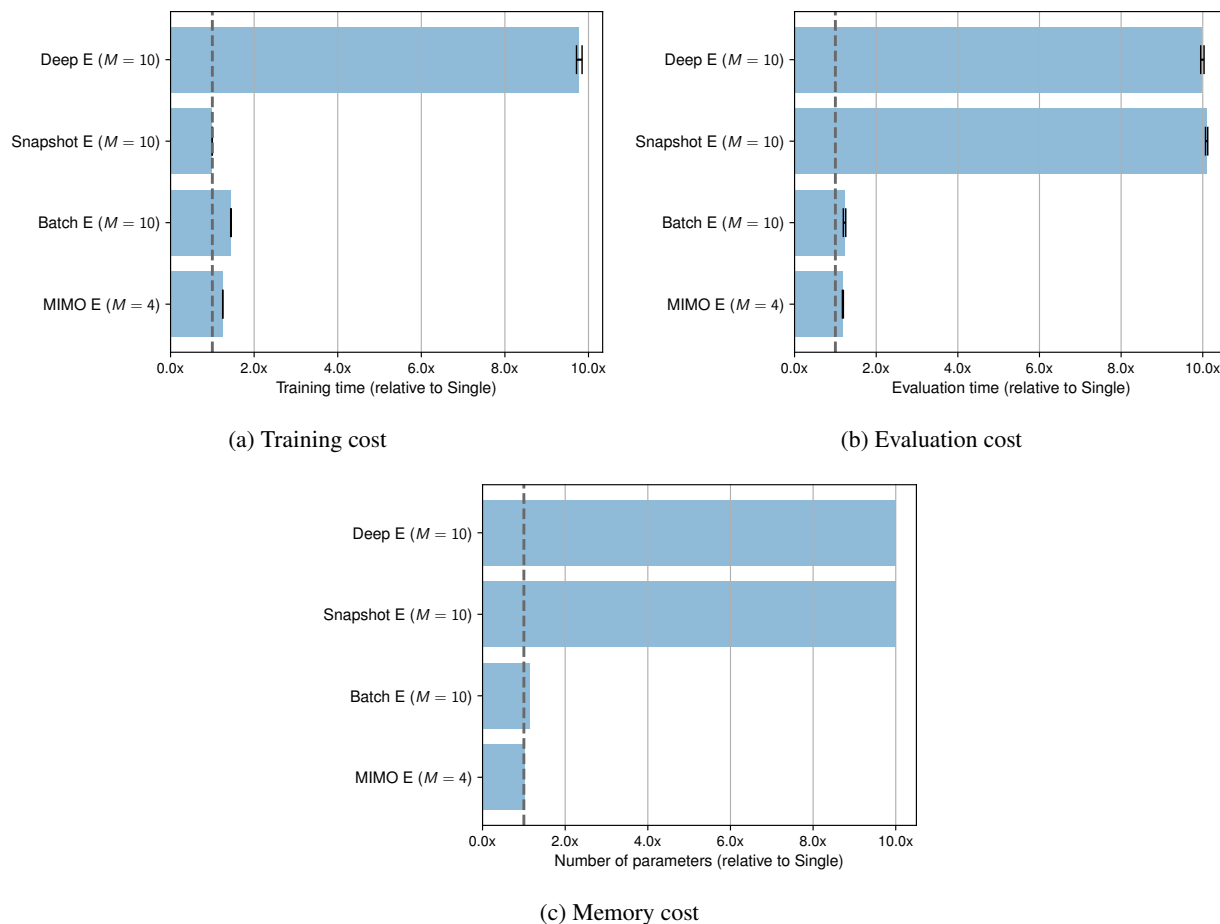


Figure 9: Training, evaluation, and memory cost

## 5.5 Computational cost

Figure 9 depicts the computational costs associated with all ensembling techniques. The values are normalized relative to the single model to facilitate easier comparisons.

In Figure 9a, the training cost is presented. The training time for the deep ensemble with  $M = 10$  members is 10 times longer than that of the single model, as it involves training 10 NNs independently. The training time for the snapshot ensemble is equivalent to that of a single model, and the number of ensemble members does not impact the training duration. Both the batch ensemble and MIMO ensemble exhibit slightly slower training times compared to the single model, with a factor of 1.5x and 1.25x, respectively. It is important to note that the batch ensemble and MIMO ensemble are trained for 25% more epochs due to a slower learning convergence.

In Figure 9b, evaluation times are presented. The deep and snapshot ensembles incur 10 times higher evaluation costs than the single NN because they require  $M = 10$  independent forward passes. Conversely, the batch ensemble and MIMO ensemble are only around 20% slower in evaluation.

Figure 9c illustrates the number of parameters stored. Memory consumption for both the deep and snapshot ensembles is 10 times higher, given the weights storage for  $M = 10$  individual NNs. The batch ensemble has approximately 10% more parameters due to the inclusion of additional fast weights. In the MIMO model, the extra parameters in the input and output layers are negligible.

In summary, the batch ensemble and MIMO ensemble incur only slight additional costs compared to the single model, making them orders of magnitude more cost-effective than the deep ensemble.

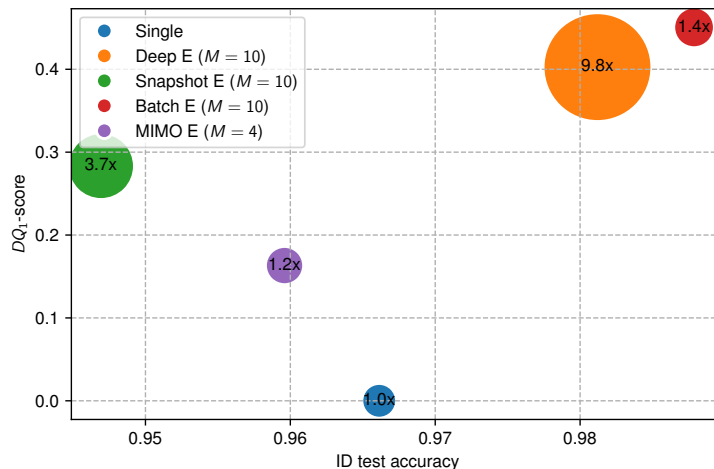


Figure 10: Accuracy on the ID set and  $DQ_1$ -score. Each point represents an ensemble model; the point size represents the weighted computational cost relative to a single NN. Models in the upper-right corner perform best

## 5.6 Cost-performance analysis

Figure 10 displays a bubble chart combining the predictive accuracy,  $DQ_1$ -scores, and computational costs of all models described in previous sections. The horizontal axis shows the test accuracy on the ID set (section 5.1), where higher scores are better. The vertical axis shows the  $DQ_1$ -scores (section 5.4), where higher scores are again better. The point size shows the weighted computational cost of the models relative to the single NN (section 5.5), with smaller points being better. Hence, optimal models are denoted by small points positioned in the upper-right corner.

To facilitate comparisons, the computational costs of each model are summarized by computing a weighted average of the three individual criteria. The criteria weights can be selected depending on the specific application at hand. For industrial parts classification, we allocate 70% weight to training time, 20% weight to evaluation time, and 10% weight to parameter count. Alternatively, in settings characterized by rapidly moving production lines, evaluation time might receive a higher weight to facilitate timely human intervention.

The plot illustrates that deep and batch ensemble significantly outperform the other models, boasting high accuracy on the ID set and high diversity quality. Batch ensemble, however, is much more computationally efficient than deep ensemble. As such, batch ensemble is a cost-effective and competitive alternative to deep ensemble. Conversely, the snapshot ensemble demonstrates decent diversity quality but has low ID accuracy, failing to match even the single NN. The MIMO ensemble lags behind the other ensembles in both aspects.

## 6 Conclusion

Reliable uncertainty estimation in NNs is crucial for their safe deployment in OR, as NNs tend to make confident yet incorrect predictions in OOD scenarios. Deep ensembles have demonstrated robust predictive performance and uncertainty estimates. However, their deployment in practice poses challenges due to substantial computational and memory requirements. This is the first study to provide a comprehensive comparison of a single NN, a deep ensemble, and three efficient NN ensembles. In addition, we propose a Diversity Quality score to quantify the ensembles' performance on the ID and OOD sets in one single metric. The efficient ensembles include a snapshot ensemble, batch ensemble, and MIMO ensemble, applied on an OR case study in industrial parts classification.

The superior performance of deep and batch ensemble over the single NN highlights the need for reliable uncertainty estimates when deploying NNs in operational settings. Furthermore, batch ensemble emerges as a cost-effective and competitive alternative to deep ensembles. It surpasses the deep ensemble both in terms of accuracy and uncertainty while demonstrating a training time speedup of 7x, a test time speedup of 8x, and 9x memory savings for ensemble size 10. Its robust uncertainty estimates are confirmed by the strong diversity quality score. Additionally, it exhibits similar uncertainty behavior when confronted with OOD data, and selecting the ensemble size is equally straightforward: the more members the better the results.

Several directions for future work are possible. Expanding studies on industrial parts classification to datasets containing more object classes would validate the findings and better simulate real-world industrial scenarios. Furthermore, ensembles hold potential in various other OR domains. For instance, in tasks like household waste sorting or quality control within production plants, the emergence of new product types or failure modes requires reliable uncertainty in classifiers.

## Acknowledgments

The authors would like to thank Thomas Suys for his contributions during his master’s thesis. This study was supported by the Research Foundation Flanders (FWO) (grant number 1S97022N).

## References

- Manu Madhav, Suhas Suresh Ambekar, and Manoj Hudnurkar. Weld defect detection with convolutional neural network: an application of deep learning. *Annals of Operations Research*, pages 1–24, 2023.
- Gary Mena, Kristof Coussemment, Koen W De Bock, Arno De Caigny, and Stefan Lessmann. Exploiting time-varying rfm measures for customer churn prediction with deep neural networks. *Annals of Operations Research*, pages 1–23, 2023.
- Chuan Guo, Geoff Pleiss, Yu Sun, and Kilian Q Weinberger. On calibration of modern neural networks. In *International Conference on Machine Learning*, pages 1321–1330. PMLR, 2017.
- Arthur Thuy and Dries F Benoit. Explainability through uncertainty: Trustworthy decision-making with neural networks. *European Journal of Operational Research*, 2023. doi:10.1016/j.ejor.2023.09.009.
- Yaniv Ovadia, Emily Fertig, Jie Ren, Zachary Nado, David Sculley, Sebastian Nowozin, Joshua Dillon, Balaji Lakshminarayanan, and Jasper Snoek. Can you trust your model’s uncertainty? evaluating predictive uncertainty under dataset shift. *Advances in neural information processing systems*, 32, 2019.
- Gao Huang, Yixuan Li, Geoff Pleiss, Zhuang Liu, John E Hopcroft, and Kilian Q Weinberger. Snapshot ensembles: Train 1, get m for free. *arXiv preprint arXiv:1704.00109*, 2017. doi:10.48550/arXiv.1704.00109.
- Yeming Wen, Dustin Tran, and Jimmy Ba. Batchensemble: an alternative approach to efficient ensemble and lifelong learning. *arXiv preprint arXiv:2002.06715*, 2020. doi:10.48550/arXiv.2002.06715.
- Marton Havasi, Rodolphe Jenatton, Stanislav Fort, Jeremiah Zhe Liu, Jasper Snoek, Balaji Lakshminarayanan, Andrew M Dai, and Dustin Tran. Training independent subnetworks for robust prediction. *arXiv preprint arXiv:2010.06610*, 2020. doi:10.48550/arXiv.2010.06610.
- Philippe Du Jardin. Forecasting bankruptcy using biclustering and neural network-based ensembles. *Annals of Operations Research*, 299(1-2):531–566, 2021. doi:10.1007/s10479-019-03283-2.
- Shaoze Cui, Dujuan Wang, Yunqiang Yin, Xin Fan, Lalitha Dhamocharan, and Ajay Kumar. Carbon trading price prediction based on a two-stage heterogeneous ensemble method. *Annals of Operations Research*, pages 1–25, 2022. doi:10.1007/s10479-022-04821-1.
- Xingmin Zhang, Zhiyong Li, Yiming Zhao, and Lan Wang. Carbon trading and covid-19: a hybrid machine learning approach for international carbon price forecasting. *Annals of Operations Research*, pages 1–29, 2023. doi:10.1007/s10479-023-05327-0.
- Manrui Jiang, Lifen Jia, Zhensong Chen, and Wei Chen. The two-stage machine learning ensemble models for stock price prediction by combining mode decomposition, extreme learning machine and improved harmony search algorithm. *Annals of Operations Research*, pages 1–33, 2022. doi:10.1007/s10479-020-03690-w.
- Fan Zhang, Hasan Fleyeh, and Chris Bales. A hybrid model based on bidirectional long short-term memory neural network and catboost for short-term electricity spot price forecasting. *Journal of the Operational Research Society*, 73(2):301–325, 2022. doi:10.1080/01605682.2020.1843976.
- Yiheng Li and Weidong Chen. Entropy method of constructing a combined model for improving loan default prediction: A case study in china. *Journal of the Operational Research Society*, 72(5):1099–1109, 2021. doi:10.1080/01605682.2019.1702905.
- Christopher Krauss, Xuan Anh Do, and Nicolas Huck. Deep neural networks, gradient-boosted trees, random forests: Statistical arbitrage on the s&p 500. *European Journal of Operational Research*, 259(2):689–702, 2017. doi:10.1016/j.ejor.2016.10.031.

- Mohammad Zoynul Abedin, Mahmudul Hasan Moon, M Kabir Hassan, and Petr Hajek. Deep learning-based exchange rate prediction during the covid-19 pandemic. *Annals of Operations Research*, pages 1–52, 2021. doi:10.1007/s10479-021-04420-6.
- Hirad Baradaran Rezaei, Alireza Amjadian, Mohammad Vahid Sebt, Reza Askari, and Abolfazl Gharaei. An ensemble method of the machine learning to prognosticate the gastric cancer. *Annals of Operations Research*, 328(1):151–192, 2023. doi:10.1007/s10479-022-04964-1.
- H Yang, WD Li, KX Hu, YC Liang, and YQ Lv. Deep ensemble learning with non-equivalent costs of fault severities for rolling bearing diagnostics. *Journal of Manufacturing Systems*, 61:249–264, 2021. doi:10.1016/j.jmsy.2021.09.009.
- Zengyuan Wu, Caihong Zhou, Fei Xu, and Wengao Lou. A cs-adaboost-bp model for product quality inspection. *Annals of Operations Research*, 308:685–701, 2022. doi:10.1007/s10479-020-03798-z.
- Joshy Easaw, Yongmei Fang, and Saeed Heravi. Using polls to forecast popular vote share for us presidential elections 2016 and 2020: An optimal forecast combination based on ensemble empirical model. *Journal of the Operational Research Society*, 74(3):905–911, 2023. doi:10.1080/01605682.2022.2101951.
- P Zicari, G Folino, M Guarascio, and L Pontieri. Combining deep ensemble learning and explanation for intelligent ticket management. *Expert Systems with Applications*, 206:117815, 2022. doi:10.1016/j.eswa.2022.117815.
- Katia Maria Poloni, Ricardo José Ferrari, and Alzheimer’s Disease Neuroimaging Initiative. A deep ensemble hippocampal cnn model for brain age estimation applied to alzheimer’s diagnosis. *Expert Systems with Applications*, 195:116622, 2022. doi:10.1016/j.eswa.2022.116622.
- Muhammad Bilal and Lukumon O Oyedele. Big data with deep learning for benchmarking profitability performance in project tendering. *Expert Systems with Applications*, 147:113194, 2020. doi:10.1016/j.eswa.2020.113194.
- Rupesh Gupta, Vatsala Anand, Sheifali Gupta, and Deepika Koundal. Deep learning model for defect analysis in industry using casting images. *Expert Systems with Applications*, page 120758, 2023. doi:10.1016/j.eswa.2023.120758.
- Rapeepan Pitakaso, Surajet Khonjun, Natthapong Nanthasamroeng, Chawis Boonmee, Chutchai Kaewta, Prem Enkvetchakul, Sarayut Gonwirat, Peerawat Chokanat, Ganokgarn Jirasirilerd, and Thanatkij Srichok. Gamification design using tourist-generated pictures to enhance visitor engagement at intercity tourist sites. *Annals of Operations Research*, pages 1–33, 2023. doi:10.1007/s10479-023-05590-1.
- Balaji Lakshminarayanan, Alexander Pritzel, and Charles Blundell. Simple and scalable predictive uncertainty estimation using deep ensembles. *Advances in neural information processing systems*, 30, 2017.
- Armen Der Kiureghian and Ove Ditlevsen. Aleatory or epistemic? does it matter? *Structural safety*, 31(2):105–112, 2009. doi:10.1016/j.strusafe.2008.06.020.
- Stefan Depeweg, Jose-Miguel Hernandez-Lobato, Finale Doshi-Velez, and Steffen Udfluft. Decomposition of uncertainty in bayesian deep learning for efficient and risk-sensitive learning. In *International Conference on Machine Learning*, pages 1184–1193. PMLR, 2018.
- Te Han and Yan-Fu Li. Out-of-distribution detection-assisted trustworthy machinery fault diagnosis approach with uncertainty-aware deep ensembles. *Reliability Engineering & System Safety*, 226:108648, 2022. doi:10.1016/j.ress.2022.108648.
- Jihyo Kim, Jiin Koo, and Sangheum Hwang. A unified benchmark for the unknown detection capability of deep neural networks. *Expert Systems with Applications*, 229:120461, 2023. doi:10.1016/j.eswa.2023.120461.
- Salvin Sanjesh Prasad, Ravinesh Chand Deo, Nathan James Downs, David Casillas-Pérez, Sancho Salcedo-Sanz, and Alfio Venerando Parisi. Very short-term solar ultraviolet-a radiation forecasting system with cloud cover images and a bayesian optimized interpretable artificial intelligence model. *Expert Systems with Applications*, 236:121273, 2024. doi:10.1016/j.eswa.2023.121273.
- Long Wen, Xiaotong Xie, Xinyu Li, and Liang Gao. A new ensemble convolutional neural network with diversity regularization for fault diagnosis. *Journal of Manufacturing Systems*, 62:964–971, 2022. doi:10.1016/j.jmsy.2020.12.002.
- Qiling Zou and Suren Chen. Resilience-based recovery scheduling of transportation network in mixed traffic environment: A deep-ensemble-assisted active learning approach. *Reliability Engineering & System Safety*, 215:107800, 2021. doi:10.1016/j.ress.2021.107800.
- Mathias Kraus, Stefan Feuerriegel, and Asil Oztekin. Deep learning in business analytics and operations research: Models, applications and managerial implications. *European Journal of Operational Research*, 281(3):628–641, 2020. ISSN 0377-2217. doi:10.1016/j.ejor.2019.09.018. Featured Cluster: Business Analytics: Defining the field and identifying a research agenda.
- Michael Zhu and Suyog Gupta. To prune, or not to prune: exploring the efficacy of pruning for model compression. *arXiv preprint arXiv:1710.01878*, 2017. doi:10.48550/arXiv.1710.01878.

- Qiwei Hu, Salem Chakhar, Sajid Siraj, and Ashraf Labib. Spare parts classification in industrial manufacturing using the dominance-based rough set approach. *European Journal of Operational Research*, 262(3):1136–1163, 2017. doi:10.1016/j.ejor.2017.04.040.
- Qiwei Hu, Yongsheng Bai, Jianmin Zhao, and Wenbin Cao. Modeling spare parts demands forecast under two-dimensional preventive maintenance policy. *Mathematical Problems in Engineering*, 2015, 2015. doi:10.1155/2015/728241.
- Ricardo Ernst and Morris A Cohen. Operations related groups (orgs): a clustering procedure for production/inventory systems. *Journal of Operations Management*, 9(4):574–598, 1990. doi:10.1016/0272-6963(90)90010-B.
- Xiaomeng Zhu, Talha Bilal, Pär Mårtensson, Lars Hanson, Mårten Björkman, and Atsuto Maki. Towards sim-to-real industrial parts classification with synthetic dataset. In *Proceedings of the IEEE/CVF Conference on Computer Vision and Pattern Recognition*, pages 4453–4462, 2023. doi:10.1109/CVPRW59228.2023.00468.
- Zachary Nado, Neil Band, Mark Collier, Josip Djolonga, Michael W Dusenberry, Sebastian Farquhar, Qixuan Feng, Angelos Filos, Marton Havasi, and Rodolphe Jenatton. Uncertainty baselines: Benchmarks for uncertainty & robustness in deep learning. *arXiv preprint arXiv:2106.04015*, 2021. doi:10.48550/arXiv.2106.04015.
- Stanislav Fort, Huiyi Hu, and Balaji Lakshminarayanan. Deep ensembles: A loss landscape perspective. *arXiv preprint arXiv:1912.02757*, 2019. doi:10.48550/arXiv.1912.02757.
- Arthur Thuy and Dries F. Benoit. Reject, March 2024. URL <https://github.com/arthur-thuy/reject>.
- Pankaj Agrawal, Richard Borgman, John M Clark, and Robert Strong. Using the price-to-earnings harmonic mean to improve firm valuation estimates. *Journal of Financial Education*, pages 98–110, 2010.
- Marina Sokolova and Guy Lapalme. A systematic analysis of performance measures for classification tasks. *Information processing & management*, 45(4):427–437, 2009. doi:10.1016/j.ipm.2009.03.002.
- Marília Barandas, Duarte Folgado, Ricardo Santos, Raquel Simão, and Hugo Gamboa. Uncertainty-based rejection in machine learning: Implications for model development and interpretability. *Electronics*, 11(3):396, 2022. doi:10.3390/electronics11030396.

## Appendix

### Reliable uncertainty with cheaper neural network ensembles: a case study in industrial parts classification

#### A Results for MIMO with 4 and 10 ensemble members

Table 3 shows the classification accuracy and the NLL metrics on the ID set for both MIMO ensemble configurations, consisting of 4 and 10 ensemble members. The single NN is added for reference. The 10-member ensemble demonstrates superior accuracy compared to its 4-member counterpart, aligning closely with the performance of the single NN.

Table 3: Performance on the ID set (MIMO with 4 and 10 members)

Model	Accuracy (%) $\uparrow$	NLL $\downarrow$
Single	$96.61 \pm 0.18$	$0.1121 \pm 0.0039$
MIMO E ( $M = 4$ )	$95.96 \pm 0.44$	$0.1168 \pm 0.0092$
MIMO E ( $M = 10$ )	$96.51 \pm 0.23$	$0.1258 \pm 0.0088$

Figure 11 displays the NRA for both models based on the total uncertainty. The NRA curve of the 10-member ensemble exhibits a notably slower increase compared to the 4-member ensemble. As such, it performs as poorly as the single NN.

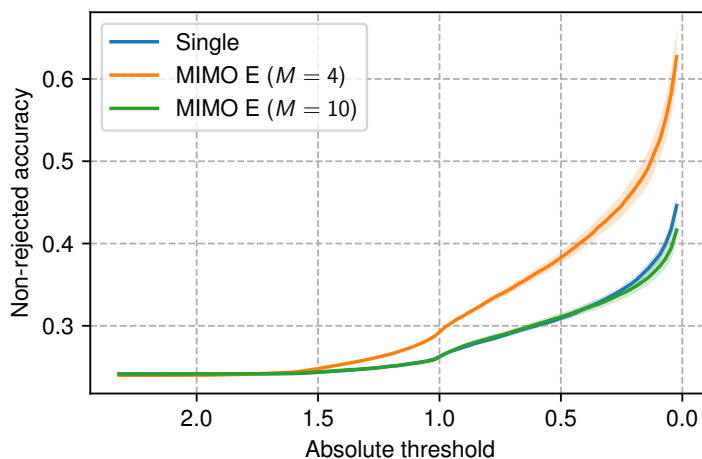


Figure 11: Non-rejected accuracy (MIMO with 4 and 10 members)

In conclusion, using the MIMO ensemble with 10 members instead of the optimal size of 3–4 reported by the authors does not seem appropriate. Although the ID accuracy is better than the 4-member configuration, the uncertainty estimates are poor, practically matching the performance of the single NN.

#### B Results with 4 ensemble members

This section presents results where all ensembles have 4 members. It is important to highlight that the MIMO ensemble is already configured with 4 members in the main body of the manuscript. This decision was made because using 10 members would restrict the capacity of individual members too much. Therefore, the outcomes presented for the deep, batch, and snapshot ensembles are different from those in the main body.

##### B.1 In-distribution performance

Table 4 shows the classification accuracy and the NLL metrics on the ID set. The difference in performance between ensembles of 4 or 10 members is minimal. The standard error bounds of the accuracy scores intersect across all three

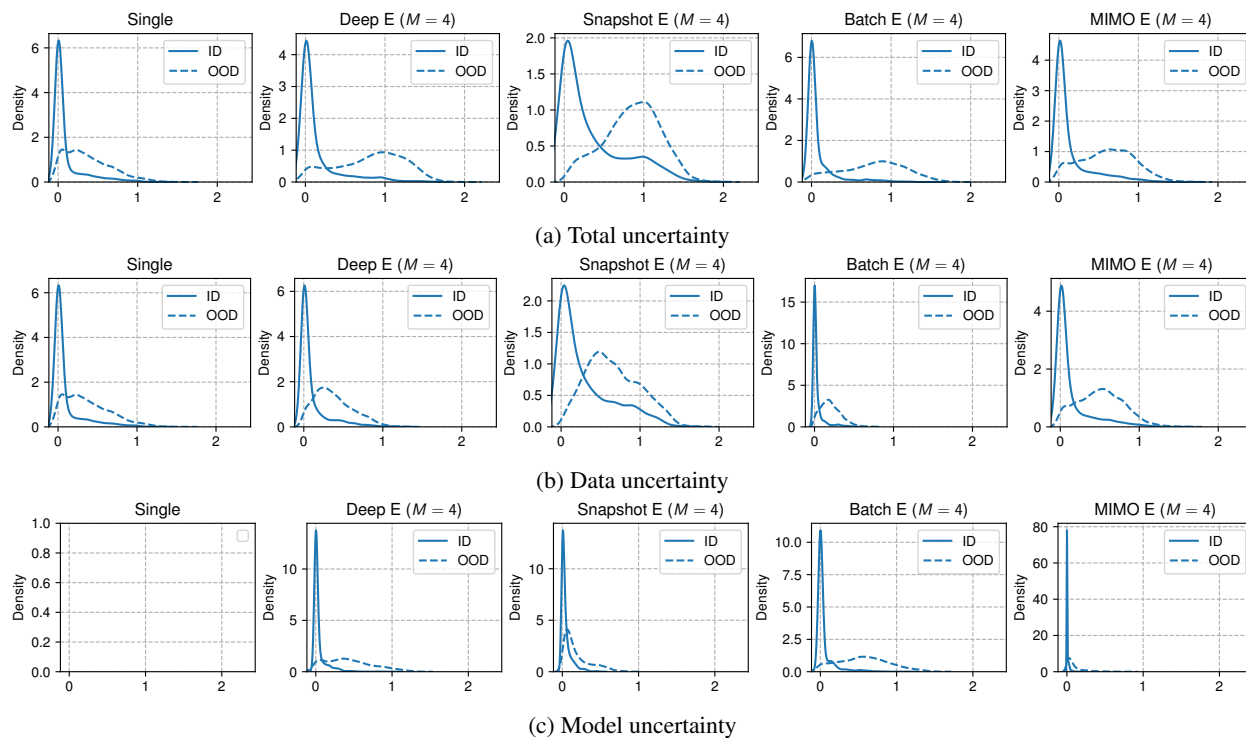


Figure 12: Densities for the data, model, and total uncertainty on the ID and OOD set (4 ensemble members)

ensembles with an adjusted ensemble size. However, batch and snapshot ensembles exhibit marginally higher NLLs. Consequently, the conclusions closely mirror those derived from configurations with 10 ensemble members. In terms of accuracy and NLL, deep ensemble outperforms the single NN, with batch ensemble even surpassing the deep ensemble. In contrast, snapshot and MIMO ensembles lag behind, performing worse than the single NN. Additionally, worth noting that while standard error margins overlap, the snapshot ensemble demonstrates slightly higher accuracy with an ensemble size of 4. Despite this marginal improvement, its performance remains inferior to that of the singular NN.

Table 4: Performance on the ID set (4 ensemble members)

Model	Accuracy (%) $\uparrow$	NLL $\downarrow$
Single	$96.61 \pm 0.18$	$0.1121 \pm 0.0039$
Deep E ( $M = 4$ )	$97.95 \pm 0.09$	$0.0748 \pm 0.0024$
Snapshot E ( $M = 4$ )	$94.97 \pm 0.25$	$0.1625 \pm 0.0051$
Batch E ( $M = 4$ )	$98.60 \pm 0.17$	$0.0586 \pm 0.0078$
MIMO E ( $M = 4$ )	$95.96 \pm 0.44$	$0.1168 \pm 0.0092$

## B.2 Uncertainty density

Figure 12 depicts the density distributions of total, data, and model uncertainty. Notably, the uncertainty levels on the ID set remain consistent with the configuration employing 10 members. Conversely, the uncertainty on the OOD set slightly lower across all three ensembles following adjustments to the ensemble size.

## B.3 Classification with rejection

Figure 13 displays the NRA for all models based on the total uncertainty. We observe a sizable decrease in NRA when transitioning from 10 ensemble members to only 4. Specifically, at lower uncertainty thresholds, both snapshot and deep ensembles exhibit a decrease of 10 percentage points, while the batch ensemble experiences a more pronounced decrease of 15 percentage points. Batch ensemble seems to be affected more by the smaller ensemble size than the

other two ensembles. Despite reaching the same NRA than MIMO at low uncertainty thresholds, the batch ensemble demonstrates consistently superior performance for moderate to larger thresholds.

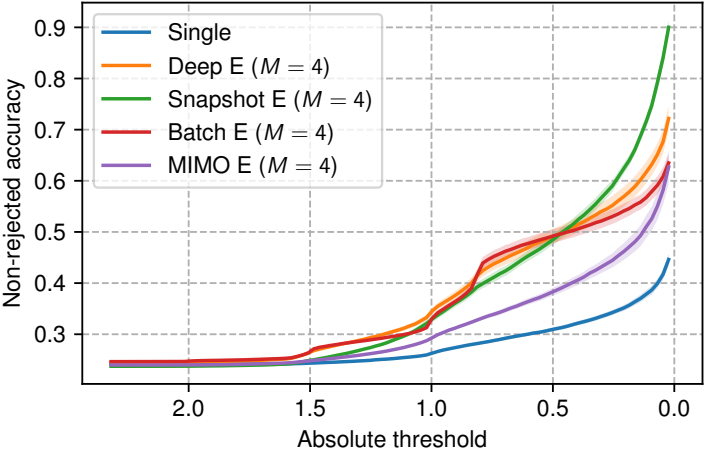


Figure 13: Non-rejected accuracy (4 ensemble members)

**B.4 Diversity analysis**

Figure 14b displays a scatterplot of diversity scores on the ID and OOD test set, where each point represents an ensemble member. The observations closely resemble those of the configuration with 10 members. However, on the OOD set, the deep ensemble is now slightly more diverse than the batch ensemble. Overall, the deep and batch ensemble are still superior over the other ensembles.

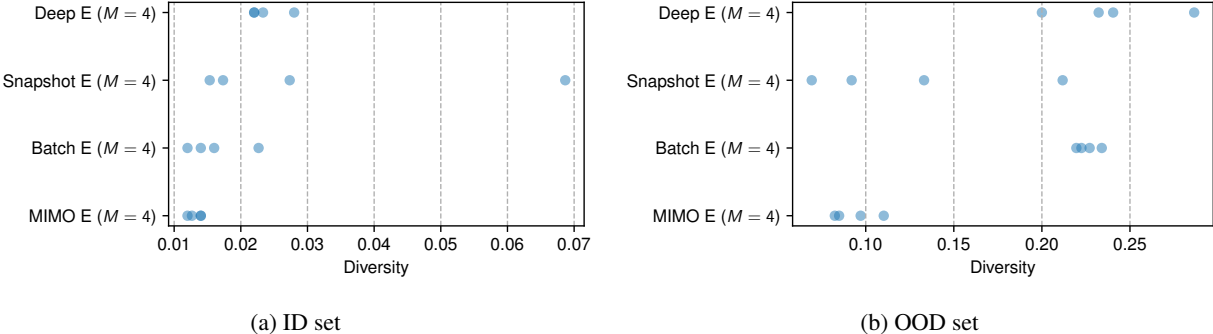


Figure 14: Diversity on the ID and OOD set (4 ensemble members). Each point represents the diversity of a trained model against the model averaged over all members

Figure 15 shows the  $DQ_1$ -scores, where each point represents an ensemble member. The observations are in line with the configuration with 10 members and follow closely on the diversity analysis in section B.4. The deep ensemble members have slightly higher  $DQ_1$ -scores than the batch ensemble, both still outperforming the snapshot and MIMO ensemble.

**B.5 Computational cost**

Figure 16 depicts the computational costs of the ensembling techniques. The values are normalized relative to the single model. As anticipated, the computational cost of the deep ensemble maintains a linear relationship with the ensemble size. Additionally, the training time of the snapshot ensemble remains consistent with that of the single NN, while its evaluation time and memory cost align with those of the deep ensemble. Conversely, the costs associated with the batch and MIMO ensembles show minimal reduction, resulting in costs that are only marginally higher than those

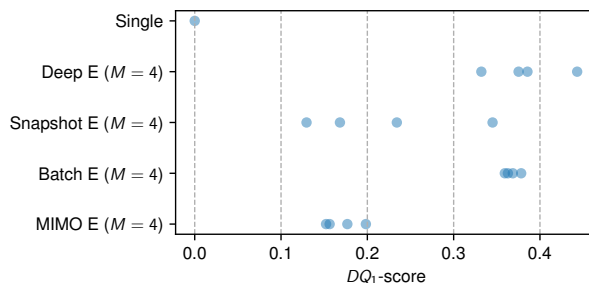


Figure 15:  $DQ_1$ -scores (4 ensemble members). Each point represents the  $DQ_1$ -score of an ensemble member

of the single NN. Consequently, using a batch ensemble with an increased ensemble size is an interesting option, as performance typically improves with larger ensemble sizes.

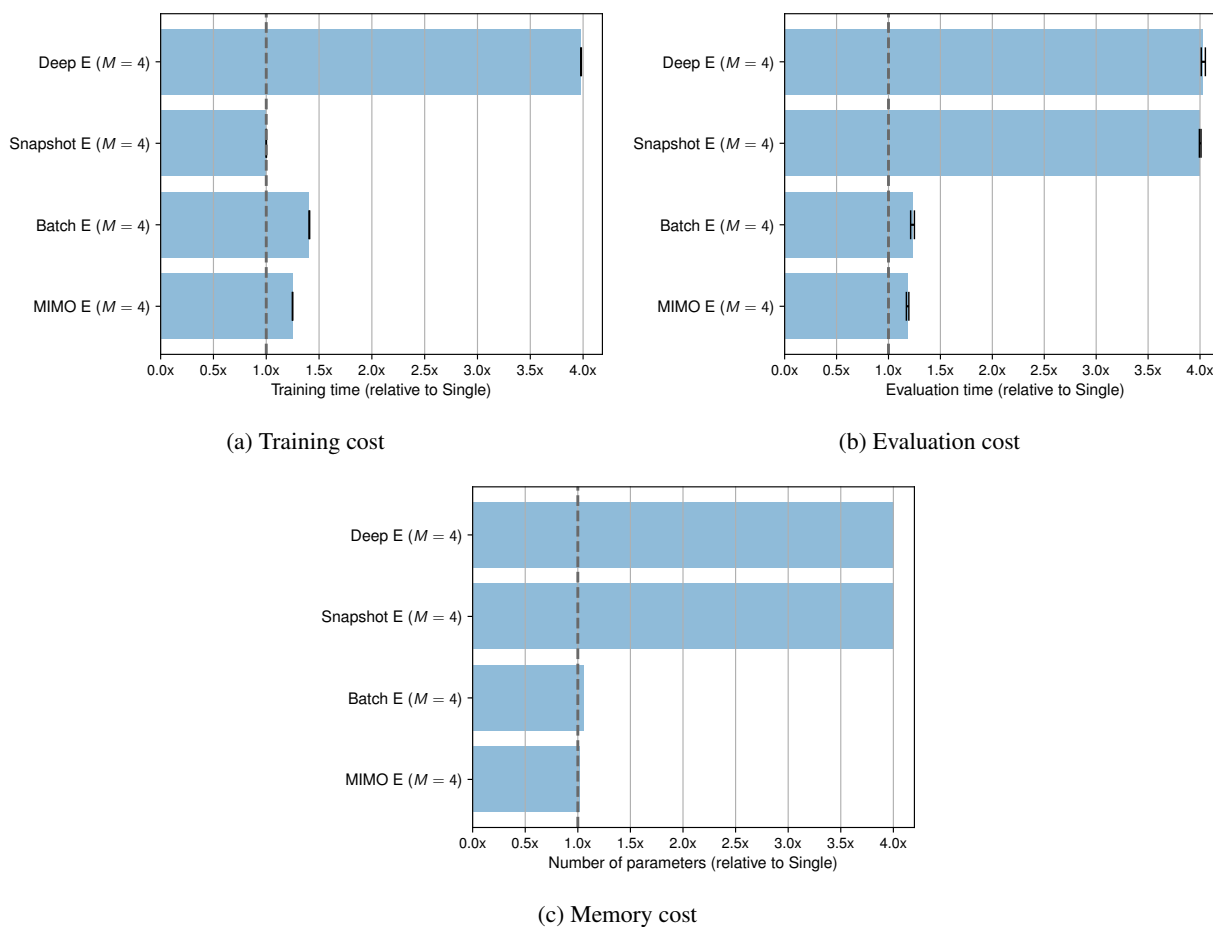


Figure 16: Training, evaluation, and memory cost (4 ensemble members)

## B.6 Cost-performance analysis

Figure 17 displays a bubble chart combining the predictive accuracy, diversity scores, and computational costs of all models described in previous sections. The observations closely resemble those of the configuration with 10 members. Deep and batch ensemble significantly outperform the other models, showcasing much higher ID accuracy and OOD diversity. Batch ensemble is still substantially more efficient than deep ensemble and is an excellent alternative.

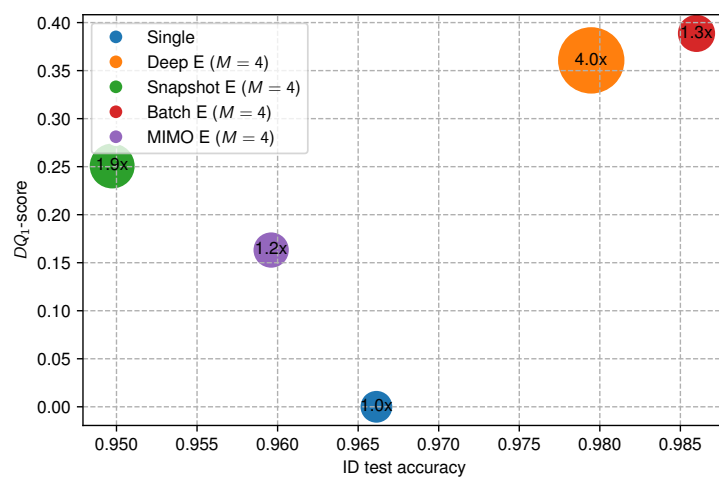


Figure 17: Accuracy on the ID set and  $DQ_1$ -score. Each point represents an ensemble model; the point size represents the weighted computational cost relative to a single NN. Models in the upper-right corner perform best